Article

Chinese Science Bulletin

Materials Science

September 2011 Vol.56 No.25: 2739–2743
doi: 10.1007/s11434-011-4597-6

The impact of nanoporous SiN_x interlayer growth position on high-quality GaN epitaxial films

MA ZiGuang*, XING ZhiGang, WANG XiaoLi, CHEN Yao, XU PeiQiang, CUI YanXiang, WANG Lu, JIANG Yang, JIA HaiQiang & CHEN Hong

Beijing National Laboratory of Condensed Matter, Institute of Physics, Chinese Academy of Sciences, Beijing 100190, China

Received February 16, 2011; accepted May 23, 2011

The impact of nanoporous SiN_x interlayer growth position on high-quality GaN epitaxial film was elucidated from the behavior of dislocations. The best quality GaN film was achieved when a nanoporous SiN_x interlayer was grown on a rough layer, with the high-resolution X-ray diffraction rocking curve full width at half maximum for $(1\bar{1}02)$ reflection decreasing to 223 arcs, and the total dislocation density reduced to less than 1.0×10^8 cm^{-2}. GaN films were grown on sapphire substrates by metal organic chemical vapor deposition. The quality of these films was investigated with high-resolution X-ray diffraction, atomic force microscopy, and cross-sectional transmission electron microscopy. A preference for the formation of half-loops to reduce threading dislocations was observed when an SiN_x interlayer was grown on a rough layer. A growth mechanism is proposed to explain this preference.

growth models, defects, metal-organic chemical vapor deposition, GaN, SiN_x

Citation: Ma Z G, Xing Z G, Wang X L, et al. The impact of nanoporous SiN_x interlayer growth position on high-quality GaN epitaxial films. Chinese Sci Bull, 2011, 56: 2739–2743, doi: 10.1007/s11434-011-4597-6

GaN and related compounds are playing an indispensable role world-wide in optoelectronic device applications, such as high-brightness light-emitting diodes (LEDs), laser diodes (LDs) and detectors, because of their large band-gaps, high thermal conductivity and chemical inertness [1,2]. However, the large density of threading dislocations (TDs) in GaN is still one of the main challenges hindering the development of nitride-based optoelectronic devices, especially for short-wavelength light-emitting devices, such as LDs and ultraviolet (UV) LEDs [3]. Generally, heteroepitaxial growth of GaN films is based on sapphire, and large dislocations are inevitably induced by the large lattice mismatch between GaN and sapphire [4]. Many efforts have been made to improve the quality of GaN grown on these substrates. Patterned template technologies such as epitaxial lateral overgrowth (ELOG), pendeo-epitaxy (PE) and lateral overgrowth from trenches (LOFT) have proved effective in dislocation reduction. These methods can reduce the dislocation density to the order of magnitude 10^5 cm^{-2} [5]. Unfortunately, contaminants are inevitably introduced into the epitaxial film by *ex-situ* lithography and etching during the entire film preparation process. Moreover, thicker GaN films are required to form well-defined smooth surfaces, which results in a more time-consuming process.

In-situ nanoporous SiN_x interlayer deposition is a much simpler and cleaner way to tailor the patterned template for GaN epitaxy. This method has been verified as a convenient and efficient way to reduce TDs to 10^7–10^8 cm^{-2} in GaN grown on sapphire substrates [6–15]. The method has been used to improve the performance of devices such as blue and green LEDs, UV-LEDs, Schottky barrier photo-detectors, and metal-semiconductor-metal photo-detectors [16–20]. However, the behavior of dislocations, including their formation, termination, threading up and bending, occur at different growth stages of GaN films. If the SiN_x interlayer was inserted at different growth stages, the quality of the

*Corresponding author (email: ziguangma@gmail.com)

GaN film would be changed because of the different effects of the SiN_x interlayer on the behavior of dislocations. However, there have been few reports on the effect of SiN_x interlayer position on the crystal quality of GaN film. In the present study the SiN_x interlayer was inserted into different stages of the GaN growth process by metal organic chemical vapor deposition (MOCVD), and the influence of different SiN_x interlayer positions on the quality of GaN was systematically investigated. Finally, GaN films with improved crystal quality and morphology were obtained when SiN_x interlayer was grown on a rough layer. The rocking curve full width at half maximum (FWHM) for the asymmetrical plane $(1\bar{1}02)$ reflection was 223 arcs and the dislocation density of the epitaxial film decreased to less than 1×10^8 cm^{-2}.

1 Materials and methods

The samples were grown on *c*-plane sapphire substrates using a modified two-step method, during which a Veeco Pioneer P125 vertical flow metal organic chemical vapor deposition (MOCVD) reactor was employed. Trimethylgallium (TMG) and ammonia (NH_3) were used as the precursors of Ga and N. Mixtures of H_2 and N_2 were used as carrier gas during the whole GaN film preparation process.

The sapphire substrate was first exposed to a hydrogen flow at 1060°C. A nominal 25 nm thick GaN nucleation layer was then deposited at 490°C, and annealed at 980°C for about 1 min. After that, a GaN layer of enhanced 3D-growth mode was grown at the same temperature, as the so-called rough layer for which the growth conditions were controlled to grow the annealed nuclei up to GaN islands that just fully covered the surface. Finally, a 2-μm high-temperature GaN layer was then grown at 1050°C to obtain a coalesced surface and high-quality epitaxial film. An *in-situ* SiN_x layer, grown for 6 min using 200 ppm silane and NH_3 under the same conditions, was inserted at various positions during GaN deposition. In samples A, B and C, SiN_x was grown on annealed sapphire substrates, on the rough layer, and on the high-temperature GaN layer with well defined surface, respectively.

The crystal qualities of these three samples were characterized by high-resolution X-ray diffraction (HRXRD) with a Bede D1 system equipped with a four-bounce channel-cut Si (220) monochromator, delivering a pure $CuK\alpha_1$ line of wavelength 0.154056 nm. The surface morphology was imaged by atomic force microscopy (AFM) with a CSPM 4000 system. Dislocations were observed with a JEOL 2010 transmission electron microscope (TEM) operating at 200 kV: the specimens were prepared by mechanical polishing followed by ion milling.

2 Results and discussion

The FWHMs of HRXRD rocking curves were determined. The symmetric (0002) and asymmetric $(1\bar{1}02)$ reflection results for the three samples are listed in Table 1. A GaN film without SiN_x interlayer was also grown using the same conditions and characterized. The FWHMs for (0002) and $(1\bar{1}02)$ of this film were 241 and 348 arcs respectively. Referring to the FWHMs in Table 1, we can conclude that the quality of the GaN film was improved by inserting an SiN_x interlayer. The FWHM for $(1\bar{1}02)$ plane of sample B was the smallest of the three samples. The 223 arcs for sample B is one of the best results that has been reported for the *in-situ* SiN_x interlayer deposition method, noting that the thickness of our sample was only 2.5 μm [12]. However, it is shown in the Table 1 that the FWHMs for the (0002) reflections of the three samples were almost the same, indicating that the influence of the SiN_x interlayer position on screw dislocation density is negligible. These (0002) and $(1\bar{1}02)$ rocking curves are related to the mosaic structure of GaN. The mosaic structures, including tilts and twists, are always accommodated by screw and edge dislocations, respectively. Consequently, the dislocation densities of the samples could be accounted for by these FWHMs for (0002) and $(1\bar{1}02)$ reflection results [21]. However, dislocation densities obtained from HRXRD measurement are always overestimated. That is due mainly to the fact that mixed dislocations which consist of the screw and edge type together are calculated repeatedly, as well as the strain influence of the tested materials and the equipment broadening from X-ray dispersion. In any case, the dislocation densities of all three samples were reduced by SiN_x interlayers, especially in the case of sample B.

To examine the surface morphology of GaN films, AFM measurements were conducted with the results shown in Figure 1(a)–(c), from which the terrace morphology on the GaN surface is clearly visible. The surface features are closely related to the presence of microstructural defects in materials [22]. The root-mean-square (RMS) roughness values in an area of 2 μm×2 μm for the three samples were 0.150, 0.095 and 0.195 nm, respectively. Thus, the AFM for sample B exhibited the best quality and morphology. To characterize the dislocation density more directly, etching was performed after growth. The surfaces of the three samples were etched in a mixture of H_3PO_4 and H_2SO_4 in mole ratio 3∶1 at 250°C for 10 min. The morphology after etching was

Table 1 FWHMs for (0002) and (1-102) planes, the root-mean-square (RMS) roughness in an area 2 μm×2 μm, and the etched pit densities for the three samples

	FWHM		RMS (nm)	Etched pit density (10^7 cm^{-2})
	(0002)	(1-102)		
Sample A	229	274	0.150	11.3
Sample B	211	223	0.092	5.5
Sample C	223	268	0.159	8.9

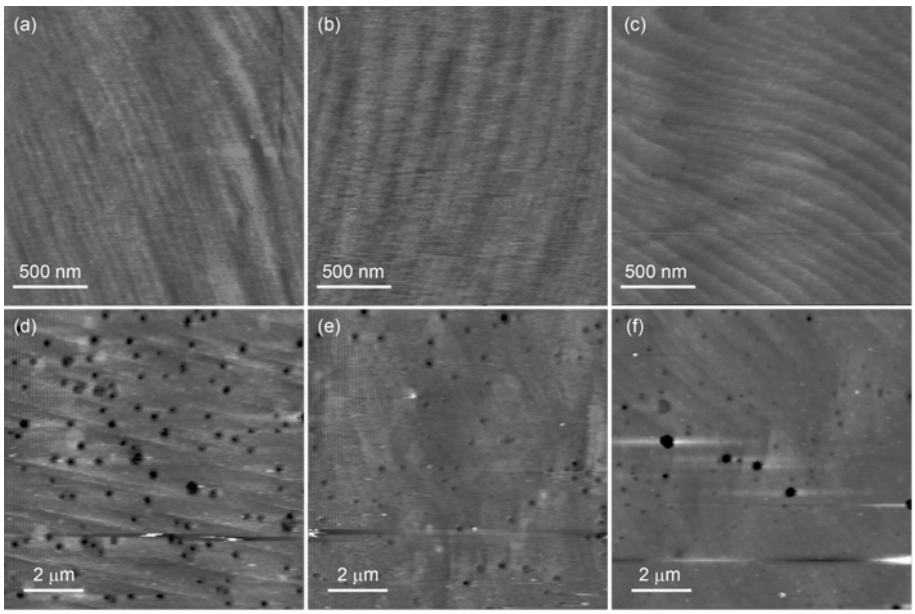

Figure 1 2 μm×2 μm AFM images of GaN surfaces: (a) For sample A, (b) for sample B, (c) for sample C; and 10 μm×10 μm AFM images after etching: (d) for sample A, (e) for sample B, (f) for sample C.

imaged by AFM as shown in Figure 1(d)–(f). The etched pit densities of the three samples are shown in Table 1: sample B had the smallest number of etched pits. The pits have been proved to originate from screw threading dislocations or mixed threading dislocations with screw components, while few pure edge dislocations cause pits [23]. Since the density of mixed dislocations is usually an order of magnitude larger than that of the screw type in GaN film, most of the pits are mixed type dislocations. The etched pit density of sample B was 5.5×10^7 cm^{-2} and the total dislocation density of sample B was less than 1×10^8 cm^{-2}.

Both AFM and HRXRD measurement revealed that the quality of sample B was superior to the quality of the other two samples, with the lowest threading dislocation density. To understand the dislocation reduction mechanism further, bright-field cross-sectional TEM analysis of samples B and C was performed. Sample A was not included because of its large threading dislocation density. Cross-sectional specimens were observed along the $[1\bar{1}00]$ direction. The images of dislocation evolution are shown in Figure 2, with a composite of some micrographs so that a panorama was obtained that can be studied systematically. The SiN_x interlayer appears as a faint line in all images. It can be observed that most of the dislocations are blocked from threading up. With the two-beam extinction: $\boldsymbol{g}\cdot\boldsymbol{b}=0$ where $\boldsymbol{g}$ is the direction of diffraction and $\boldsymbol{b}$ is the Burgers vector, the dislocations with different Burgers vectors could be out of contrast when $\boldsymbol{g}$ changed. So when $\boldsymbol{g}$=[0002], pure edge dislocations ($\boldsymbol{b}_e$=1/3$[11\bar{2}0]$) are invisible, while for $\boldsymbol{g}$=$[11\bar{2}0]$, pure screw dislocations ($\boldsymbol{b}_s$=[0001]) vanish. In both cases mixed dislocations ($\boldsymbol{b}_m$=1/3$[11\bar{2}3]$) are visible [24]. TEM images for the sample B specimen with $\boldsymbol{g}$=[0002] and $[11\bar{2}0]$ are shown in Figure 2(a) and (b), respectively, and for sample C in Figure 2(c) and (d), respectively. Comparing the images with different $\boldsymbol{g}$, some screw dislocations that are not seen in Figure 2(b) and (d) are present on the top of images as shown in Figure 2(a) and (c). Hence, it is easy to reach the conclusion that edge dislocations are more effectively stopped from threading up by the SiN_x interlayer than are screw dislocations. This is in agreement with the results of HRXRD measurement which indicate that the (0002) plane FWHMs are almost the same, while the $(11\bar{2}0)$ plane FWHMs are different. Analyzing the two specimens reveals that in sample B, except for dislocations blocked by SiN_x interlayer, many dislocations were bent towards the in-plane direction during growth. Subsequently some of them with the opposite Burgers vector were annihilated by the formation of half-loops. The result was creation of dislocation half-loops with increased probability of decreasing the threading dislocation density. These dislocation half-loops are not seen in sample C. Consequently, the effect of the SiN_x interlayer on decreasing the TD density is much more obvious in sample B than in sample C.

It is well known that a dislocation is terminated at a free surface or when it incorporates with other dislocations that have partly opposite Burgers vectors. Both of these mechanisms led to the decreased dislocation density in sample B, while for sample C only dislocations blocked from threading up were clearly seen. This is demonstrated by the sketch maps of the growing process for samples B and C in Figure 3(a) and (c), and the *in-situ* monitored reflectivity spectra in Figure 3(b) and (d), respectively. For sample B many hexangular GaN crystalline grains formed on the substrate

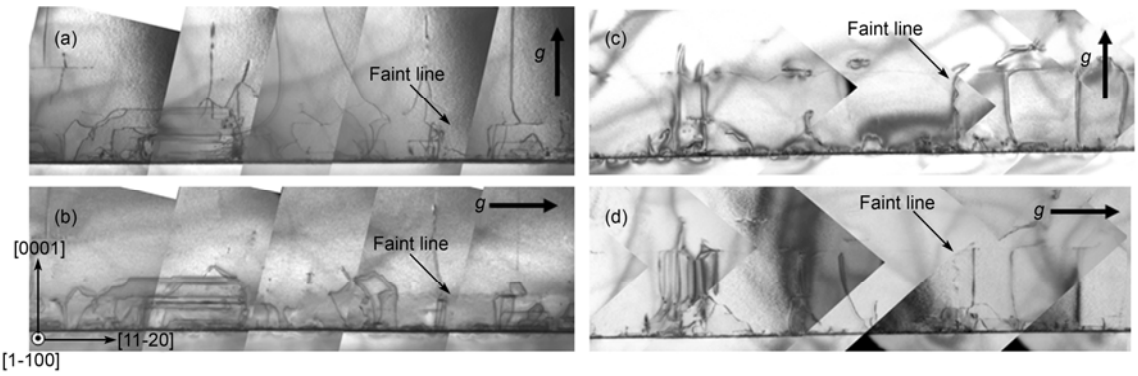

Figure 2 Bright-field cross-sectional TEM images for (a) sample B with $\boldsymbol{g}$=[0002], with screw and mixed dislocations observable; (b) sample B with $\boldsymbol{g}$=[11-20], with edge and mixed dislocations observable; (c) sample C with $\boldsymbol{g}$=[0002]; (d) sample C with $\boldsymbol{g}$=[$11\bar{2}0$]. For sample B, the threading dislocation bending can be seen at the bottom of (a) and (b). The faint lines in the images are SiN_x interlayers.

with ($1\bar{1}0h$) plane during the rough layer process. The SiN_x interlayer tends to deposit at the bottom of the rough layer among the grain boundaries to minimize the surface energy and interface energy, and only cusps of grains were not covered with a SiN_x amorphous layer. The SiN_x layer prevented the formation of dislocations at the grain boundaries, and blocked some dislocations in the grains from threading up. After SiN_x deposition, the cusps of 3D crystalline grain are overgrown laterally in conditions for GaN high-temperature growth, and the horizontal growth rate is faster as demonstrated in Figure 3(a). The shapes of the overgrown grains favor dislocation bending to the horizontal direction because of the inclined free plane, especially the ($1\bar{1}01$) plane formed during the growth process. Pairs of horizontal dislocations with partly opposite Burgers vectors will incorporate. In addition, the overgrown grains extend the time of grain coalescence because of their initially 3D shapes, which minimize the formation of dislocations at the coalescence boundary. However, this growth mode is not appropriate for sample C, for which, shortly after the high temperature growth step begins, the surface of GaN film is atomically flat. Hence the SiN_x interlayer nucleates around the outcrops of dislocations because of the stress field around the dislocations, then grows mainly with 2D growth mode covering most of the surface. The SiN_x interlayer stops many dislocations threading up, as shown in Figure 3(c). However, after SiN_x interlayer deposition, conditions for GaN high-temperature growth increase the lateral growth rate. The film coalesces promptly because of the 2D-shaped grains, which increases the probability of forming dislocations

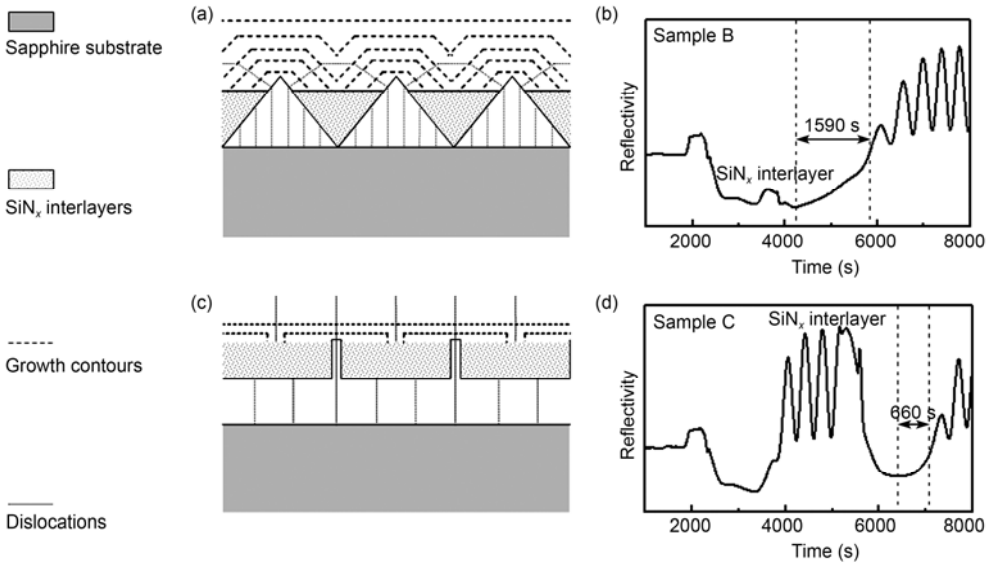

Figure 3 (a) The sketch map of growth mode for sample B; (b) *in-situ* monitored reflectivity spectrum for sample B; (c) the sketch map of growth mode for sample C; (d) *in-situ* monitored reflectivity for sample C. The SiN_x interlayer in sketch map is only a few atomic layers; it has been magnified to demonstrate the growth modes.

at the coalescence boundary. To estimate the coalescence rate, the recovery time was defined using *in-situ* monitored reflectivity from the minimal reflectivity to the reflectivity of the sapphire, as shown in Figure 3(b) and (d), respectively. It is apparent that the recovery time of sample B was longer than sample C, indicating that the grains coalesced more slowly in sample B. All of the reasons mentioned above made the dislocation density of sample B lower than that of sample C. It can also be proved that the recovery time is shorter for sample A than for sample B. Moreover, in sample A no dislocations are blocked during the growth process because the SiN_x interlayer is deposited directly on sapphire.

According to the above analysis, it can be deduced that growing an SiN_x interlayer on a rough layer formed initially more effectively decreases dislocation density than an interlayer grown on a flat surface. This is an important factor for growing high quality GaN epitaxial films, because the effect of the SiN_x interlayer on decreasing the dislocation density can be optimised provided that the rough layer is accurately controlled. Since the method is easy in practice, optimization of the SiN_x position on a rough layer could also be used with other Group III-nitride materials to decrease dislocations.

3 Conclusion

In summary, we have studied the effect of an SiN_x interlayer on the quality of GaN films, by inserting it at different growth positions during the GaN epitaxial process. The best results are obtained when SiN_x is grown on a rough layer. The preferential insertion of SiN_x on the rough layer not only blocks dislocations formed initially from threading up, but also promotes the 3D growth mode of GaN, delays the recovery time from 3D to 2D growth mode, and minimizes the probability of dislocation formation at the incorporation boundary. The dislocation density of GaN epitaxial film is successfully minimized when the growth position of SiN_x interlayer is optimized on the rough layer.

The authors gratefully acknowledge support from the National Natural Science Foundation of China (*50872146 and 60890192/F0404*) *and the Nationa Basic Research Program of China* (*2010CB327501*).

1 Gil B. Group III Nitride Semiconductor Compounds. Oxford: Clarendon, 1998
2 Nakamura S, Fasol G. The Blue Laser Diode—The Complete Story. New York: Springer, 2000
3 Wang T, Liu Y H, Lee Y B, et al. Fabrication of high performance of AlGaN/GaN-based UV light-emitting diodes. J Cryst Growth, 2002, 235: 177–182
4 Look D C, Sizelove J R. Dislocation scattering in GaN. Phys Rev Lett, 1999, 82: 1237–1240
5 Gibart P. Metal organic vapour phase epitaxy of GaN and lateral overgrowth. Rep Prog Phys, 2004, 67: 667
6 Yun F, Moon Y T, Fu Y, et al. Efficacy of single and double SiN_x interlayers on defect reduction in GaN overlayers grown by organometallic vapor-phase epitaxy. J Appl Phys, 2005, 98: 123502–123509
7 Sagar A, Feenstra R M, Inoki C K, et al. Dislocation density reduction in GaN using porous SiN interlayers. Phys Stat Sol, 2005, 202: 722–726
8 Moon Y T, Xie J, Liu C, et al. A study of the morphology of GaN seed layers on *in situ* deposited Si_xN_y and its effect on properties of overgrown GaN epilayers. J Cryst Growth, 2006, 291: 301–308
9 Xie J, Ozgur U, Fu Y, et al. Low dislocation densities and long carrier lifetimes in GaN thin films grown on a SiN*x* nanonetwork. Appl Phys Lett, 2007, 90: 041107–041109
10 Xie J Q, Chevtchenko A S, Ozgur U, et al. Defect reduction in GaN epilayers grown by metal-organic chemical vapor deposition with *in situ* SiN_x nanonetwork. Appl Phys Lett, 2007, 90: 262112–262114
11 Kappers M J, Datta R, Oliver R A, et al. Threading dislocation reduction in (0001) GaN thin films using SiN_x interlayers. J Cryst Growth, 2007, 300: 70–74
12 Bchetnia A, Toure A, Lafford T A, et al. Effect of thickness on structural and electrical properties of GaN films grown on SiN-treated sapphire. J Cryst Growth, 2007, 308: 283–289
13 Hertkorn J, Lipski F, Bruckner P, et al. Process optimization for the effective reduction of threading dislocations in MOVPE grown GaN using *in situ* deposited SiN_x masks. J Cryst Growth, 2008, 310: 4867–4870
14 Kim D K. Influence of a SiN mask on GaN layer by metalorganic chemical vapor deposition. J Mater Sci Mater Electron, 2008, 19: 471–475
15 Fang Z L, Li S P, Li J C, et al. GaN on Si-rich SiN_x-coated sapphire at different growth stages: The surface morphologies and optical properties. Thin Solid Films, 2008, 516: 6344–6352
16 Liu C H, Chuang R W, Chang S J, et al. InGaN/GaN MQW blue LEDs with GaN/SiN double buffer layers. Mater Sci Eng B, 2004, 111: 214–217
17 Xie J Q, Fu Y, Ni X F, et al. I-V characteristics of Au/Ni Schottky diodes on GaN with SiN_x nanonetwork. Appl Phys Lett, 2006, 89: 152108–152110
18 Jhou Y D, Chang S J, Su Y K, et al. GaN Schottky barrier photodetectors with SiN/GaN nucleation layer. Appl Phys Lett, 2007, 91: 103506–103508
19 Huang G S, Kuo H C, Lo M H, et al. Improvement of efficiency and ESD characteristics of ultraviolet light-emitting diodes by inserting AlGaN and SiN buffer layers. J Cryst Growth, 2007, 305: 55–58
20 Tsai C M, Sheu J K, Lai W C, et al. GaN-based LEDs output power improved by textured GaN/sapphire interface using *in situ* treatment process during epitaxial growth. IEEE J Sel Top Quantum Electron, 2009, 15: 1275–1280
21 Moram M A, Vickers M E. X-ray diffraction of III-nitrides. Rep Prog Phys, 2009, 72: 036502
22 Liu J Q, Wang J F, Liu Y F, et al. High-resolution X-ray diffraction analysis on HVPE-grown thick GaN layers. J Cryst Growth, 2009, 311: 3080–3084
23 Wen T C, Lee W I, Sheu J K, et al. Observation of dislocation etch pits in epitaxial lateral overgrowth GaN by wet etching. Solid-State Electron, 2002, 46: 555–558
24 Ponce F A, Cherns D, Young W T, et al. Characterization of dislocations in GaN by transmission electron diffraction and microscopy techniques. Appl Phys Lett, 1996, 69: 770–772